

Investigation of Cutting Edge Radius Influence on Tool Wear Using FEM Simulation in DEFORM 3D

Martin Necpal^{1,*}, Marek Vozár¹

Slovak University of Technology in Bratislava, Faculty of Material Science and technology in Trnava, Slovakia¹
martin.necpal@stuba.sk

Abstract: This article presents a study of the influence of cutting edge rounding on the wear of monolithic milling tools using the finite element method (FEM) and DEFORM 3D software. After manufacturing by grinding, monolithic milling tools have considerably sharp cutting edges that are prone to breakage and chipping. Industrial practice and cutting edge zone theory recommend edge preparation to create a defined cutting edge radius. The optimal radius value depends on the machined material, cutting conditions, and other factors, and remains unclear. This study investigates the influence of the cutting edge radius on tool wear using 3D FEM simulation with the Usui wear model, which is considered suitable for machining processes. Initial simulations with sharp cutting edges were performed to determine the sensitivity of wear predictions to the Usui model constants. Subsequently, different cutting edge radii were simulated under identical cutting conditions. The simulation results demonstrate the relationship between cutting edge radius and wear progression. The findings provide guidelines for selecting suitable cutting edge preparation parameters to minimize tool wear when milling with monolithic tools.

Keywords: CUTTING EDGE RADIUS, TOOL WEAR SIMULATION, FEM, DEFORM, USUI MODEL, MILLING

1. Introduction

Tool wear is the primary mechanism that limits tool life in milling and directly affects surface quality and machining costs [1, 2]. After grinding, monolithic milling tools have very sharp cutting edges. Industrial experience shows that such edges are prone to rapid wear and micro-chipping [3]: the geometry is mechanically unstable and cannot withstand the concentrated stresses at the cutting edge during material removal. Tool manufacturers therefore recommend edge preparation by multitude of available methods to create a controlled cutting edge radius [4].

The cutting edge radius (also called edge rounding or hone radius) affects cutting forces, heat generation, chip formation, and wear mechanisms [5]. A larger radius distributes the load over a greater contact area, improving edge stability, but also increases cutting forces and heat generation. A smaller radius keeps forces lower but leaves the edge susceptible to premature failure. The optimal value depends on workpiece material, cutting conditions, and tool material [6]. Finite element method (FEM) simulation has become standard practice for studying machining processes [7], enabling investigation of stress and temperature distributions in the cutting zone that are difficult to measure directly. Several commercial packages support machining simulation, including DEFORM, AdvantEdge, and Abaqus [8].

Tool wear prediction in FEM simulation requires a wear model. The Usui wear model is commonly used for this purpose [9]. This model relates wear rate to interface variables:

$$\frac{dW}{dt} = A \cdot \sigma_n \cdot v_s \cdot \exp\left(-\frac{B}{T}\right) \quad (1)$$

where W is wear depth, σ_n is normal stress, v_s is sliding velocity, T is interface temperature, and A and B are material constants that must be calibrated [10]. This study investigates the influence of cutting edge radius on tool wear in milling using 3D FEM simulation in DEFORM. First, the Usui wear model is calibrated using simulations with a sharp cutting edge. The sensitivity of wear predictions to constants A and B is analyzed. Then, simulations with three different cutting edge radius (5 μm , 15 μm , and 45 μm) are performed to determine the optimal radius for minimal wear. Inner layer means higher accuracy, but longer production time).

2. Materials and Methods

2.1. Simulation setup

The FEM simulations were performed using DEFORM software. Two simulation approaches were used: 2D simulations for Usui wear model calibration with a sharp cutting edge, and 3D simulations for investigation of different cutting edge radius. The 2D calibration model is defined identically to the 3D wear model in

terms of material properties, constitutive models, and cutting conditions. The dimensional reduction to 2D was chosen solely to reduce computation time during calibration. The only variable between the 3D simulations is the cutting edge radius; all other parameters remain constant.

The cutting tool geometry was derived from the commercial SECO Tools JS754 100E2C.0Z4-HXT end mill. The tool material is cemented carbide grade CTS20D, which corresponds to ISO classification K20–K40. The tool was modeled as a rigid body, which is standard practice in machining FEM when tool deformation is negligible compared to workpiece deformation. Consequently, only thermal properties are assigned to the tool material (Table 1). The method used to extract the 2D and 3D model geometry from the commercial tool follows the same principle as described in [17].

Table 1: Thermal properties of the tool material (carbide, rigid body).

	Value	Unit
Thermal conductivity	59	$\text{Wm}^{-1}\text{K}^{-1}$
Specific heat	290	J/Kg.K
Density	15 600	Kg.m^{-3}

The workpiece material behavior was described by the Johnson-Cook constitutive model [11, 12]:

$$\bar{\sigma} = (A + B\bar{\epsilon}^n) \left(1 + C \ln \frac{\dot{\bar{\epsilon}}}{\dot{\bar{\epsilon}}_0}\right) \left(1 - \left(\frac{T - T_{room}}{T_{melt} - T_{room}}\right)^m\right) \quad (2)$$

where $\bar{\sigma}$ is the equivalent flow stress, $\bar{\epsilon}$ is the equivalent plastic strain, $\dot{\bar{\epsilon}}$ is the equivalent strain rate, $\dot{\bar{\epsilon}}_0$ is the reference strain rate, T is temperature, T_{room} is room temperature, and T_{melt} is the melting temperature. The constants A , B , n , C , and m characterize the workpiece material. The workpiece material was AISI316L. Johnson-Cook constants and thermal properties for the workpiece are listed in Table 2.

Table 2: Workpiece material Johnson-Cook constants and thermal properties

	Symbol	Value	Unit
Yield stress	A	310.8	MPa
Strain hardening coefficient	B	881.38	MPa
Strain hardening exponent	n	0.178	-
Strain rate sensitivity	C	0.19	-
Thermal softening exponent	m	1.25	-
Thermal conductivity		18.9	$\text{Wm}^{-1}\text{K}^{-1}$
Specific heat		500	J/Kg.K
Density		8000	Kg.m^{-3}

The 3D simulation setup is shown in Figure 1. To reduce computational demands, the model was simplified by representing only a segment of the tool containing the main cutting edge rather than the full tool geometry. This allows the simulation to capture the cutting mechanics and chip formation without excessive computation time.

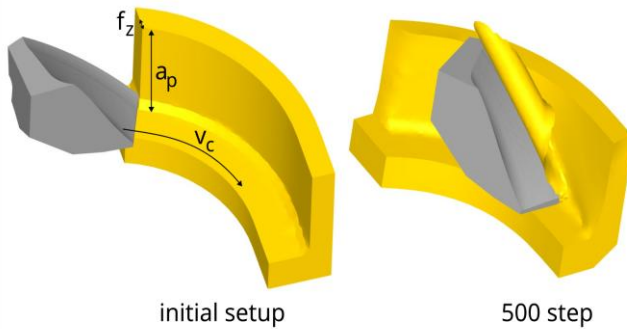


Fig. 1 3D FEM simulation setup in DEFORM: simplified model showing the main cutting edge segment and chip formation

The cutting conditions were kept constant for all simulations (Table 3):

Table 3: Thermal properties of the tool material (carbide, rigid body).

Cutting Parameter	Symbol	Value	Unit
Cutting speed	v_c	190	m/min
Feed per tooth	f_z	0.09	mm
Axial depth	a_p	3	mm
Radial depth	a_e	3	mm

2.2. Tool geometry and cutting edge radius

The monolithic milling tool geometry was modeled according to standard tool parameters. A sharp edge (as-ground condition, radius $< 2 \mu\text{m}$) was used exclusively in the 2D calibration model. Following cutting edge radii sizes were investigated in the 3D wear simulations: $r_n = 5, 15, \text{ and } 45 \mu\text{m}$. Figure 2 shows the FEM mesh of the tool with the three edge radius configurations.

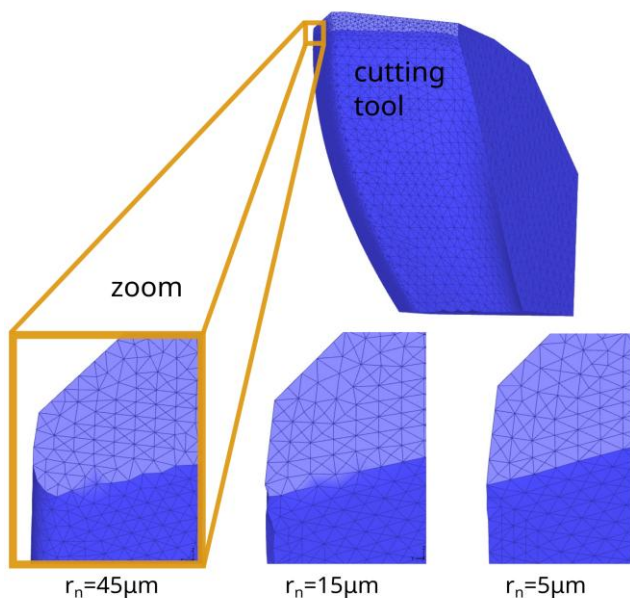


Fig. 2 Edge radius configurations: $r_n = 5, 15, \text{ and } 45 \mu\text{m}$.

2.3. Usui wear model calibration

The Usui wear model (Equation 1) requires calibration of constants A and B. These constants depend on the tool-workpiece material combination and must be determined experimentally or through inverse analysis [13]. Binder et al. [14] applied a similar

calibration procedure for coated carbide tools in turning, showing that constant selection strongly affects predicted wear.

Due to the substantially lower computational cost compared to 3D simulation, calibration was performed using 2D simulations of milling with a sharp cutting edge. Three combinations of constants were evaluated, as summarized in Table 4.

Table 4: Tested Usui constant and resulting wear rates from 2d calibration simulation

No.	A	B	Wear
1	1×10^{-7}	2000	$6.7 \times 10^{-3} \text{ m} \cdot \text{m}^{-3} \cdot \text{s}^{-1}$
2	1×10^{-8}	2500	$3 \times 10^{-4} \text{ mm}^{-3} \cdot \text{s}^{-1}$
3	1×10^{-9}	3000	$1 \times 10^{-5} \text{ mm}^{-3} \cdot \text{s}^{-1}$

Cutting speed was held constant throughout the calibration. Although varying cutting speed would provide broader validation of the constants, the available experimental data for sharp cutting edge wear were obtained under constant cutting conditions, which constrained the calibration accordingly.

2.4. Simulation procedure

The simulation procedure consisted of two phases. In the calibration phase, a 2D FEM model with a sharp cutting edge was constructed and simulations were run with different combinations of constants A and B. Wear distribution and depth were analyzed and the constants that best matched available experimental reference data were selected for further use.

In the edge radius investigation phase, the calibrated Usui constants were applied to three 3D models with cutting edge radius of 5, 15, and 45 μm . All simulations were run under identical cutting conditions and wear development was compared across the three configurations.

3. Result and Discussion

3.1. Calibration result

The 2D calibration simulations with a sharp cutting edge showed clear sensitivity of predicted wear to both Usui constants (Table 4). Increasing A by one order of magnitude from 10^{-8} to 10^{-7} increased the wear rate by more than twenty times. Decreasing A to 10^{-9} produced negligible wear, inconsistent with experimental observations for sharp cutting edges.

Based on comparison with experimental results for sharp cutting edge wear and in agreement with values reported in the literature [14], the constants $A = 10^{-8}$ and $B = 2500$ were selected, yielding a wear rate of $0.0003 \text{ m}^3 \cdot \text{s}^{-1}$. These calibrated constants were applied to all subsequent 3D simulations of the cutting edge radius influence.

3.2. Influence of cutting edge radius on wear

Using the calibrated Usui model, simulations were performed for the three edge radius. Figure 3 shows the wear distribution on the tool rake face for each configuration.

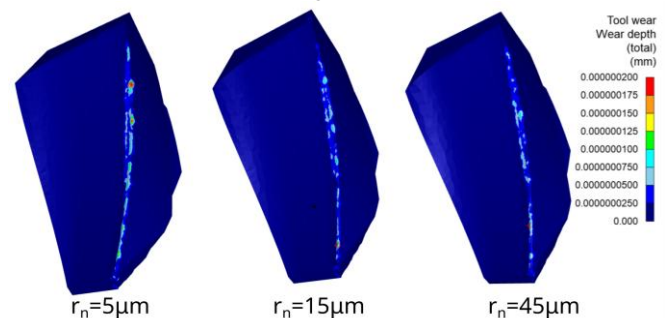


Fig. 3 Wear distribution on cutting edge

The results show that cutting edge radius affects both the location and magnitude of maximum wear. Key simulation output

variables extracted from the DEFORM results are compared in Table 5.

Table 5: Simulation output variables for the tree cutting edge radius

Parameter	$R_n=45\mu\text{m}$	$R_n=15\mu\text{m}$	$R_n=5\mu\text{m}$	Unit
Sl. velocity flank	3240	3240	3240	mms^{-1}
Sl. velocity rake	2025	2025	2025	mms^{-1}
Max interface press.	25.7	18.2	17.7	GPa
Max wear rate	2.46×10^{-3}	3.86×10^{-3}	5.66×10^{-3}	$\text{mm}^3 \text{s}^{-1}$
Max wear dept	121	116	241	μm

Interface pressure increases with radius (17.7 to 25.7 GPa), as the blunter edge enlarges the contact zone and raises local contact stress. Despite this, the wear rate decreases with increasing radius: the sharp 5 μm edge produces the highest wear rate (0.00566 mm^3/s) because heat concentrates in a small volume at the tip, driving the exponential term in the Usui model. Maximum wear depth shows the clearest separation — 241 μm at 5 μm versus 116 and 121 μm at 15 and 45 μm — with the 15 μm radius offering the best overall result.

3.3. Analysis of wear mechanism

The wear mechanism shifts with edge radius. At 5 μm , stress and heat concentrate at the tip, producing rapid localized removal and the deepest wear (241 μm). At 15 μm , the thermal load spreads over a wider contact zone (Figure 4), yielding the lowest wear depth (116 μm) and a moderate wear rate — a balance between edge strength and contact pressure. At 45 μm , the larger contact area raises interface pressure to 25.7 GPa, promoting ploughing and resulting in wear depth (121 μm) comparable to the 15 μm case but under significantly higher stress, indicating less efficient edge geometry.

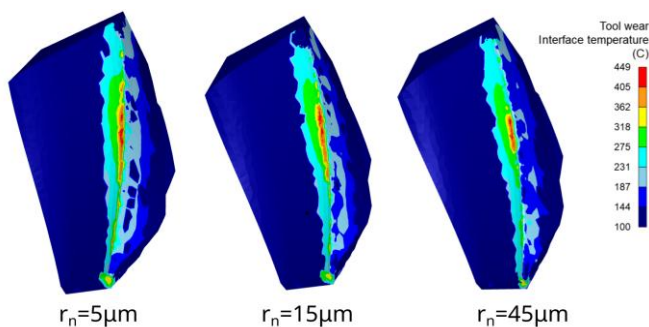


Fig. 4 Temperature distribution on cutting edge for different edge radius

3. Discussion

Figure 5 shows a comparison between the experimentally observed wear land on the cutting tool (left) and the numerically simulated tool wear (right) for identical cutting conditions as those used in the dissertation by Vozár [16].

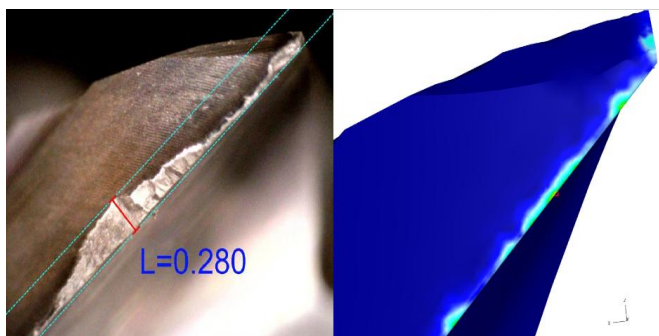


Fig. 5 Comparison of the experimentally observed worn cutting tool (left) and numerically simulated tool wear (right) under identical cutting conditions as in the dissertation by Vozár [16].

The FEM results show that cutting edge radius affects tool wear in milling. The Usui wear model, after proper calibration, can predict wear trends for different edge geometries. The calibration phase showed that both constants A and B must be carefully selected. Small changes in these values produce large differences in predicted wear. Calibration against experimental data is therefore necessary. Limitations of this study include the simplified tool geometry, the assumptions inherent in the Johnson-Cook material model, and the use of a single set of cutting conditions. Future work should extend the investigation to multiple cutting speeds and feed rates, and validate simulation results against experimentally measured wear data.

4. Conclusion

This study investigated the influence of cutting edge radius on tool wear in milling using 3D FEM simulation in DEFORM. The Usui wear model requires careful calibration of constants A and B. The 2D calibration simulations demonstrated high sensitivity to both parameters, with a one-order-of-magnitude change in A altering the predicted wear rate by more than twenty times. The constants $A = 10^{-8}$ and $B = 2500$, yielding a wear rate of 0.0003, were found to best match the available reference data and were applied to all subsequent 3D simulations.

Cutting edge radius affects both the distribution and magnitude of wear on the rake face. The as-ground sharp edge showed increased tool wear and higher temperature concentrations along the cutting edge. Among the tested radii of 5, 15, and 45 μm , the 15 μm radius size produced the lowest wear depth under the investigated cutting conditions. The optimal cutting edge radius is a compromise between edge stability and cutting performance. Based on the simulation results, a radius of approximately 15 μm is recommended for the investigated tool-workpiece combination. The FEM approach demonstrated here can inform edge preparation decisions ahead of experimental trials, shortening the development cycle for monolithic milling tools.

Acknowledge

This work was supported by the Slovak Research and Development Agency under the contract No. APVV-21-0071. This work was supported by the Science Grant Agency - project VEGA 1/0266/23.

References

1. Y. Altintas, Manufacturing Automation (Cambridge Univ. Press, 2012)
2. V.P. Astakhov, Tribology of Metal Cutting (Elsevier, 2006)
3. B. Denkena, D. Biermann, CIRP Ann. 63, 631 (2014)
4. C.J.C. Rodriguez, Cutting edge preparation (PhD Thesis, Kassel Univ., 2009)
5. C.F. Wyen, K. Wegener, CIRP Ann. 59, 93 (2010)
6. T. Özel, T.K. Hsu, E. Zeren, Int. J. Adv. Manuf. Technol. 25, 262 (2005)
7. P.J. Arrazola et al., CIRP Ann. 62, 695 (2013)
8. DEFORM User Manual (Scientific Forming Technologies Corp., Columbus, OH, 2023)
9. E. Usui, T. Shirakashi, T. Kitagawa, Wear 100, 129 (1984)
10. Y.C. Yen et al., J. Mater. Process. Technol. 146, 82 (2004)
11. G.R. Johnson, W.H. Cook, Proc. 7th Int. Symp. Ballistics, 541 (1983)
12. S.P.F.C. Jaspers, J.H. Dautzenberg, J. Mater. Process. Technol. 122, 322 (2002)
13. A. Attanasio et al., CIRP Ann. 57, 61 (2008)
14. M. Binder, F. Klocke, D. Lung, Wear 330-331, 600 (2015)
15. N.E. Karkalos, A.P. Markopoulos, Procedia Manuf. 22, 107 (2018)
16. M. Vozár, Influence of cutting edge microgeometry (Dissertation, STU Bratislava, 2022)
17. M. Neechal, T. Vopát, M. Vozár, Acta Tech. Napoc. 67(1s) (2024)